Optical spectra of CdSe nanocrystals under hydrostatic pressure

2001 J. Phys.: Condens. Matter 13 2033

(http://iopscience.iop.org/0953-8984/13/9/327)

INSTITUTE OF PHYSICS PUBLISHING JOURNAL OF PHYSICS: CONDENSED MATTER

J. Phys.: Condens. Matter **13** (2001) 2033–2043 www.iop.org/Journals/cm PII: S0953-8984(01)16930-4

Optical spectra of CdSe nanocrystals under hydrostatic pressure

Jingbo Li[1], Guo-Hua Li[1], Jian-Bai Xia[1], Jing-bo Zhang[2], Yuan Lin[2] and Xu-rui Xiao[2]

[1] National Laboratory for Superlattices and Microstructures, Institute of Semiconductors, Chinese Academy of Sciences, PO Box 912, Beijing 100083, People's Republic of China
[2] Centre of Molecular Sciences, Institute of Chemistry, Chinese Academy of Sciences, Beijing 100080, People's Republic of China

Received 7 September 2000

Abstract

Optical spectra of CdSe nanocrystals are measured at room temperature under pressure ranging from 0 to 5.2 GPa. The exciton energies shift linearly with pressure below 5.2 GPa. The pressure coefficient is 27 meV GPa^{-1} for small CdSe nanocrystals with the radius of 2.4 nm. With the approximation of a rigid-atomic pseudopotential, the pressure coefficients of the energy band are calculated. By using the hole effective-mass Hamiltonian for the semiconductors with wurtzite structure under various pressures, we study the exciton states and optical spectra for CdSe nanocrystals under hydrostatic pressure in detail. The intrinsic asymmetry of the hexagonal lattice structure and the effect of spin–orbit coupling on the hole states are investigated. The Coulomb interaction of the exciton states is also taken into account. It is found that the theoretical results are in good agreement with the experimental values.

1. Introduction

Recent advances in colloidal chemical techniques (CCT) have made possible the fabrication of semiconductor nanocrystals or quantum dots (QDs) with very high quality. There have been quite a lot of theoretical and experimental studies [1–20] on the interesting features of their electronic structure and optical properties. The most striking property of semiconductor QDs is the massive change in optical properties as a function of quantum dot size, which renders them attractive candidates for application as tunable light absorbers and emitters in optoelectronic devices. Other properties such as the melting temperature [6] and solid–solid phase transition [7–10] have also been found to change with varying size of the nanocrystals. The above variation of fundamental properties is achieved by reducing the size of the nanocrystal, not by altering its chemical composition.

For semiconductors of finite size, it is well known that quantum confinement has dramatic effects on the electronic structure of nanocrystals. High pressure leads to more closely packed structure, which provides another way to alter the electronic state of semiconductors. In

0953-8984/01/092033+11$30.00

consequence, it is interesting to study the electronic structure and optical properties when one introduces both a quantum confinement effect and high pressure in semiconductors. In the last decade, Alivisatos *et al* [3] investigated the electronic and vibrational properties of CdSe nanocrystals at high pressure. Then Zhao *et al* [4] measured pressure-tuned resonant Raman scattering and photoluminescence in CdS nanocrystals. Recently Tolbert *et al* [7–9] studied the size dependence of structural transformations in CdSe nanocrystals by using high-pressure x-ray diffraction and high-pressure optical absorption at room temperature. It is found that the nanocrystals undergo a transition from wurtzite to rock-salt structure analogous to that observed in bulk CdSe. One of the present authors [11] reported pressure-induced Γ–X crossover in InAs/GaAs quantum dots. Menoni *et al* [12] presented the first experimental evidence showing that strong quantum confinement significantly reduces the separation between direct and indirect conduction band states in InP. In addition, they applied hydrostatic pressure to further modify the electronic structure and reveal the indirect states at high pressure. Chen *et al* [13,14] investigated the photoluminescence of self-assembled $In_{0.55}Al_{0.45}As/Al_{0.5}Ga_{0.5}As$ quantum dots grown on (311)A GaAs substrates under high pressure, and demonstrated that the QDs have a type-II structure with an X valley as the lowest conduction level. As regards theoretical study, only for bulk materials composed of II–VI compounds under high pressure have the electronic structure and structural transitions been calculated, by using the pseudopotential method [15]. Zunger's group [16] have investigated the quantum-size effects on the pressure-induced transition from direct to indirect band gaps in InP quantum dots. However, to our knowledge there have been few works studying the linear pressure properties of CdSe nanocrystals by using photoluminescence measurements. Furthermore, it is worthwhile to introduce theoretical work to explain the linear pressure coefficient of II–VI nanocrystals in detail.

The nanocrystallite QDs of II–VI compounds are usually embedded in large-band-gap matrixes, such as glasses, polymers, liquids, rock salts, or zeolites. For CdSe, CdS, and ZnS nanocrystallites the common lattice structure is hexagonal (wurtzite), as proved by high-resolution TEM and x-ray diffraction [19]. However, the above-cited theoretical works using the effective-mass model were mainly based on a Hamiltonian with zinc-blende structure [18–20], or treated the crystal-field splitting (due to the hexagonal structure) as a perturbation [21–25]. Recently Efros *et al* [22] have considered the crystal shape asymmetry and the intrinsic crystal field (hexagonal) within the framework of a quasicubic model, and obtained optically passive ('dark-exciton') and optically active ('bright-exciton') states for CdSe QDs. The theoretical results are in agreement with the size dependence of the Stokes shifts obtained in fluorescence line-narrowing and photoluminescence experiments for CdSe nanocrystals. In reference [26] we derived the hole effective-mass Hamiltonian for the semiconductors with wurtzite structure. The energies and corresponding wave functions are calculated with the effective-mass Hamiltonian obtained for the CdSe QDs. Our numerical results are in agreement with the experiment and the 'dark-exciton' theory.

In this paper we synthesize nearly monodisperse CdSe nanocrystals by using a variation of a technique developed by Murray *et al* [19]. The size dependences of the optical spectra for the CdSe nanocrystals are measured at room temperature under pressure ranging from 0 to 5.2 GPa. The exciton energies shift linearly with pressure below 5.2 GPa. The pressure coefficient is 27 meV GPa^{-1} for small CdSe nanocrystals with the radius of 2.4 nm. With the approximation of a rigid-atomic pseudopotential, the pressure coefficients of the energy band are calculated. We developed a second-order-tensors model [18, 26–28] to study the spherical quantum dots. By using the hole effective-mass Hamiltonian for the semiconductors with wurtzite structure under various pressures, we study the exciton states and optical spectra of CdSe nanocrystals under hydrostatic pressure in detail. The intrinsic asymmetry of the hexagonal lattice structure and the effect of spin–orbit coupling (SOC) on the hole states are

investigated. The Coulomb interaction of the exciton states is also taken into account. It is found that the theoretical results are in good agreement with the experimental values.

The remainder of the paper is organized as follows. We describe the experiment in section 2. In section 3 we present the calculation method for the system being considered. Our experimental and numerical results are given in section 4. Finally, we briefly give our conclusions in section 4.

2. Experiments

We adapted the methods of references [2] and [19], and modified them to synthesize the nanocrystalline CdSe as follows. A 0.02 g sample of Se was dissolved in 1 g of tributyl-phosphine (TBP). To this solution 0.05 g of dimethyl-cadmium was added. 0.4 ml of the resulting solution was added into 10 g tri-*n*-octylphosphine oxide (TOPO) at 340 °C, under N_2; immediately the solution was removed from the heat and allowed to cool to room temperature under N_2. The nanocrystalline CdSe powder was obtained by separating and purifying the solution with methanol and toluene.

Using this procedure, we prepared two samples. One was a solution with toluene for use in the optical spectra measurement under high pressure. The other was homogeneously dispersed in a PMMA film with a thickness between 50 and 100 μm for use in the AFM measurement.

Figure 1(a) shows an AFM image of the uncapped sample. It is found that the CdSe nanocrystals are nearly spherical with mean radius about 2.4 nm. The samples used in the experiment are found to have an average size dispersion of $\sigma = 6.4\%$ (see figure 1(b)).

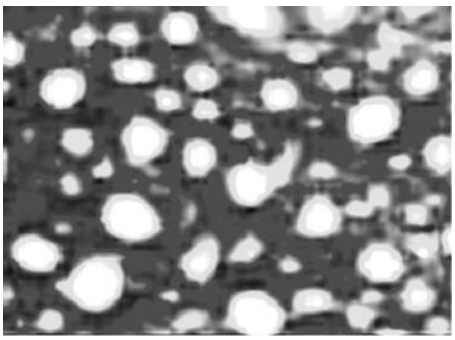

(a)

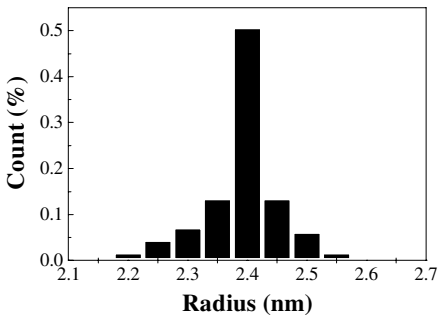

(b)

Figure 1. (a) An AFM image of CdSe nanocrystals. (b) The size distribution.

The photoluminescence (PL) was measured at 300 K using the 488.0 nm line of an Ar^+ laser as the source of excitation with power density of about 10^4 W cm^{-2}. The emitted light is dispersed by a JY-HRD2 monochromator and detected by a photomultiplier. The hydrostatic pressure was generated by a diamond anvil cell (DAC) with a 4:1 methanol–ethanol mixture as the pressure-transmitting medium. The pressure was monitored by means of the spectral shift of the ruby R_1 line.

3. Model and calculation

3.1. Wurtzite-type Hamiltonian

The hole effective-mass Hamiltonian for wurtzite semiconductors was derived for the case of zero SOC [26, 27, 29]:

$$H = \frac{1}{2m_0}\begin{vmatrix} Lp_x^2 + Mp_y^2 + Np_z^2 & Rp_xp_y & Ap_0p_x + Qp_xp_z \\ Rp_xp_y & Lp_y^2 + Mp_x^2 + Np_z^2 & Ap_0p_y + Qp_yp_z \\ Ap_0p_x + Qp_xp_z & Ap_0p_y + Qp_yp_z & S(p_x^2 + p_y^2) + Tp_z^2 + 2m_0\Delta_c \end{vmatrix} \tag{1}$$

where the basis functions are X-like, Y-like (Γ_6), and Z-like (Γ_1) functions, $L, M, \ldots, S, T$ are effective-mass parameters, and Δ_c is the crystal-field splitting energy. For the II–VI compounds such as CdS, ZnS, CdSe, the Γ_6 energy levels of the valence band are higher than the Γ_1 energy level, so Δ_c is greater than zero (hereafter we take the negative hole energy as positive as shown in equation (1)). The effective-mass parameters are determined by fitting the energy bands near the valence band top to those calculated by the empirical pseudopotential method as in reference [26]. The form factors of the atomic pseudopotentials are fitted with Cohen's formula [30]:

$$V(G) = \frac{v_1(G^2 - v_2)}{e^{v_3(G^2 - v_4)} + 1} \tag{2}$$

where v_1, v_2, v_3, v_4 are empirical parameters determined from the experimental energy values or *ab initio* theoretically calculated values at some special points of the Brillouin zone. The unit of G is au^{-1}.

3.2. The rigid-atomic pseudopotential approximation

In this paper we assume that the pseudopotential of a solid is composed of atomic pseudopotentials and that every atomic pseudopotential is unchanged under hydrostatic pressure [31].

The lattice constant decreases when the hydrostatic pressure applied to the nanocrystals increases. The relation between the pressure P and the lattice constant a (or c) can be described by the Murnaghan equation of state

$$P = \frac{B_0}{B_0'}\left[\left(\frac{a_0}{a}\right)^{3B_0'} - 1\right] \tag{3}$$

where B_0 is the bulk modulus, B_0' is the derivative of B_0 with respect to P, and a_0 is the lattice constant without application of pressure.

If the pressure is not too high, equation (3) is approximated by a linear equation:

$$P = \frac{B_0}{B_0'}\left[\left(\frac{a_0}{a_0 + \Delta a}\right)^{3B_0'} - 1\right] = \frac{B_0}{B_0'}\left[\left(\frac{1}{1 + \Delta a/a_0}\right)^{3B_0'} - 1\right] \approx -B_0\frac{3\Delta a}{a_0}. \tag{4}$$

3.3. Electronic structure of spherical quantum dots

From the effective-mass parameters for hexagonal semiconductors [26], we see that the conduction band for electrons is strictly not isotropic, with different effective masses in the z-direction and x, y-direction. The effective-mass Hamiltonian of the electron is written as

$$H_e = \frac{1}{2m_x}(p_x^2 + p_y^2) + \frac{1}{2m_z}p_z^2 \tag{5}$$

where m_x and m_z are the effective masses in the x- (or y-) and z-directions, respectively.

From reference [26] we see that for II–VI compounds the difference between m_x and m_z is so small that we can consider l and m to be good quantum numbers, where l and m are the orbital angular momentum and its z-component, respectively. The eigen-energy of the electron state $C_{ln}j_l(k_n^l r)$ is

$$E_{l,n} = \frac{\hbar^2}{2m_a}\left(\frac{\alpha_n^l}{R}\right)^2 \tag{6}$$

where $j_l(x)$ is the spherical Bessel function of lth order, $\alpha_n^l = k_n^l R$ is the nth zero point of j_l, R is the radius of the sphere, $C_{l,n}$ is the normalization constant,

$$C_{l,n} = \frac{\sqrt{2}}{R^{3/2}}\frac{1}{j_{l+1}(\alpha_n^l)}.$$

When the basis functions of the valence band top are

$$|11\rangle = \frac{1}{\sqrt{2}}(X + \mathrm{i}Y) \qquad |10\rangle = Z \qquad |1\,{-1}\rangle = \frac{1}{\sqrt{2}}(X - \mathrm{i}Y)$$

with components of angular momentum 1, 0, and -1, respectively, the hole effective-mass Hamiltonian (1) in the zero-SOC limit can be written as

$$H_h = \frac{1}{2m_0}\begin{vmatrix} P_1 & S & T \\ S^* & P_3 & S \\ T^* & S^* & P_1 \end{vmatrix} \tag{7}$$

where

$$\begin{aligned}
P_1 &= \gamma_1 p^2 - \sqrt{\frac{2}{3}}\gamma_2 P_0^{(2)} \\
P_3 &= \gamma_1' p^2 + 2\sqrt{\frac{2}{3}}\gamma_2' P_0^{(2)} + 2m_0\Delta_c \\
T &= \eta P_{-2}^{(2)} + \delta P_2^{(2)} \\
T^* &= \eta P_2^{(2)} + \delta P_{-2}^{(2)} \\
S &= A p_0 P_{-1}^{(1)} + \sqrt{2}\gamma_3' P_{-1}^{(2)} \\
S^* &= -A p_0 P_1^{(2)} - \sqrt{2}\gamma_3' P_1^{(2)}.
\end{aligned}$$

$P^{(2)}$, $P^{(1)}$ are the second-order and first-order tensors of the momentum operator, respectively. The effective-mass parameters γ_1, γ_2, ... are related to L, M, N, ... as follows:

$$\begin{aligned}
&\gamma_1 = \frac{1}{3}(L + M + N) && \gamma_2 = \frac{1}{6}(L + M - 2N) && \gamma_3 = \frac{1}{6}R \\
&\gamma_1' = \frac{1}{3}(T + 2S) && \gamma_2' = \frac{1}{6}(T - S) && \gamma_3' = \frac{1}{6}Q \\
&\eta = \frac{1}{6}(L - M + R) && \delta = \frac{1}{6}(L - M - R).
\end{aligned}$$

$L, M, \ldots, S, T$ are effective-mass parameters for hexagonal semiconductors, and are taken from reference [26].

For the same basis functions, the SOC Hamiltonian is written as [26–28]

$$H_{SO} = \begin{vmatrix} -\lambda & 0 & 0 & 0 & 0 & 0 \\ 0 & 0 & 0 & \sqrt{2}\lambda & 0 & 0 \\ 0 & 0 & \lambda & 0 & -\sqrt{2}\lambda & 0 \\ 0 & \sqrt{2}\lambda & 0 & \lambda & 0 & 0 \\ 0 & 0 & -\sqrt{2}\lambda & 0 & 0 & 0 \\ 0 & 0 & 0 & 0 & 0 & -\lambda \end{vmatrix} \tag{8}$$

where the first three basis functions correspond to spin up, and the second three basis functions correspond to spin down. Also,

$$\lambda = \frac{\hbar^3}{4m_0^2c^2}\langle X|(\partial V/\partial x)\,\partial/\partial y|Y\rangle = \frac{\Delta_{SO}}{3} \tag{9}$$

and Δ_{SO} is the spin–orbit-splitting energy.

The eigen-energies and corresponding eigenstates in the quantum spheres are calculated as in references [26–28]. The wave functions are expanded in spherical Bessel functions and spherical harmonic functions for the zero-SOC case:

$$\Psi_h = \sum_{l,n} \begin{pmatrix} a_{l,n}C_{l,n}j_l(k_n^l r)Y_{l,m-1}(\theta,\phi) \\ b_{l,n}C_{l,n}j_l(k_n^l r)Y_{l,m}(\theta,\phi) \\ d_{l,n}C_{l,n}j_l(k_n^l r)Y_{l,m+1}(\theta,\phi) \end{pmatrix}. \tag{10}$$

Because of the hexagonal symmetry, only the z-component of the angular momentum J_z is a good quantum number. The first-order tensor operator terms in the Hamiltonian (7), derived from the linear terms of the momentum operator in Hamiltonian (1), couple the states of even angular momentum l and odd l; the summation over l in the expansion of wave function (10) includes both even and odd l, unlike in the case of zinc-blende semiconductors. In that case, the summation over l includes either even l or odd l due to the second-order tensor operators.

In the finite-SOC case we start from the hole Hamiltonian (7) for both spin-up states and spin-down states, to which we add the SOC Hamiltonian (8), and we keep the z-component of the total angular momentum as a constant. For example, if we take $J_z = 0$ in equation (10) for the first three basis functions, then we take $J_z = 1$ in equation (10) for the second three basis functions, in order for the z-component of the total angular momentum to be 1/2.

3.4. Exciton states

If we take the electronic Bohr radius $a_e^* = \hbar^2\epsilon_r/m_e^*e^2$, and the Rydberg $R_e^* = m_e^*e^4/2\hbar^2\epsilon_r^2$ (m_e^* is the effective mass of the electron in units of the free-electron mass m_0, and ϵ_r is the dielectric constant of the materials) as the units of length and energy, the exciton Hamiltonian in a quantum sphere can be written as

$$H = H_0 + V_{e-h} \tag{11}$$

$$H_0 = H_e + H_h + H_{SO} + V_e(r) + V_h(r) \tag{12}$$

$$V_{e-h} = -\frac{2}{r_{eh}} \tag{13}$$

where e (h) refers to electrons (holes) respectively, V_e (V_h) is the confined potential barrier of electrons (holes). V_{e-h} is the term describing the Coulomb interaction between the electrons and holes.

The exciton wave function can be expanded in terms of the electron wave function and the hole wave function:

$$\Psi_{ex} = \sum_{i,j} c_{ij} \Psi_{ei}(r_e) \Psi_{hj}(r_h) \tag{14}$$

where $\Psi_{ei}(r_{ei})$ and $\Psi_{hj}(r_{hj})$ are the wave functions of the electronic and hole eigenstates, respectively. The matrix element of the Coulomb interaction can be calculated by using

$$\frac{1}{r_{eh}} = \sum_{k=0}^{\infty} \frac{r_<^k}{r_>^{k+1}} P_k(\cos\theta_{eh}) \tag{15}$$

$$P_k(\cos\theta_{eh}) = \frac{4\pi}{2k+1} \sum_{m=-k}^{k} Y_{km}^*(\theta_e, \varphi_e) Y_{km}(\theta_h, \varphi_h) \tag{16}$$

where the P_k are the Legendre polynomials, θ_{eh} is the angle between the position vector of the electron (r_e) and the hole (r_h), $r_< \equiv \min(r_e, r_h)$, and $r_> \equiv \max(r_e, r_h)$ [27, 35].

The exciton energy can be obtained from the secular equation

$$|(E_{n_e,l_e} + E_{m_h,l_h} - E)\delta_{ij} + V_{ij}| = 0. \tag{17}$$

The matrix element of the Coulomb interaction V_{ij} is given by

$$\left\langle \frac{1}{r_{eh}} \right\rangle = \sum_{l,k} R^k \frac{4\pi}{2k+1} \sum_{m=-k}^{k} (-1)^m \langle Y_{l'_e m'_e} | Y_{k-m} | Y_{l_e m_e} \rangle \langle Y_{l'_h m'_h} | Y_{km} | Y_{l_h m_h} \rangle \tag{18}$$

where

$$R^k = \sum_{l} \int_0^{\infty} \int_0^{\infty} R_e(n_e, l_e, m_e) R_e(n'_e, l'_e, m'_e) R_h(n_h, l_h, m_h) R_e(n'_h, l'_h, m'_h) \times \frac{r_<^k}{r_>^{k+1}} r_e^2 r_h^2 \, \mathrm{d}r_e \, \mathrm{d}r_h \tag{19}$$

$$\begin{aligned} \langle Y_{l'm'} | Y_{km} | Y_{lm} \rangle &= \int_0^{2\pi} \int_0^{\pi} Y_{l'm'}(\theta, \varphi) Y_{km}(\theta, \varphi) Y_{lm}(\theta, \varphi) \sin(\theta) \, \mathrm{d}\theta \, \mathrm{d}\varphi \\ &= \left[\frac{(2l'+1)(2l+1)(2k+1)}{4\pi} \right]^{1/2} \begin{pmatrix} k & l_h & l'_h \\ 0 & 0 & 0 \end{pmatrix} \begin{pmatrix} k & l_h & l'_h \\ m & m_h & m'_h \end{pmatrix}. \end{aligned} \tag{20}$$

4. Results and discussion

The room temperature PL spectra are shown in figure 2. The luminescence intensities have been normalized according to the strongest peak. The measurements were made at room temperature and with relatively high excitation intensity; thus both excitonic and band-to-band transitions may contribute to the luminescence. The values of the hydrostatic pressure applied in the measurements are marked in the figure. The sharp line at 2.37 eV is a Raman line from the diamond anvils. With increasing pressure the shape of the spectra remains similar, but it is shifted to higher energies. The band-to-band PL emission is broadened with a full width at half-maximum (FWHM) ∼120 meV, reflecting the size distribution of the colloidally grown CdSe QDs. For III–V QDs [11, 13, 14] or superlattices [32], an X-like state would shift to lower energy with increasing pressure, and Γ–X mixing [11,13,14] is more important for small QDs. However, in our present study of II–VI QDs there is no evidence of an X-like state or Γ–X mixing. The luminescence peak in figure 2 has a blue-shift with increasing pressure and we identify it as arising from E^{Γ}-related transitions.

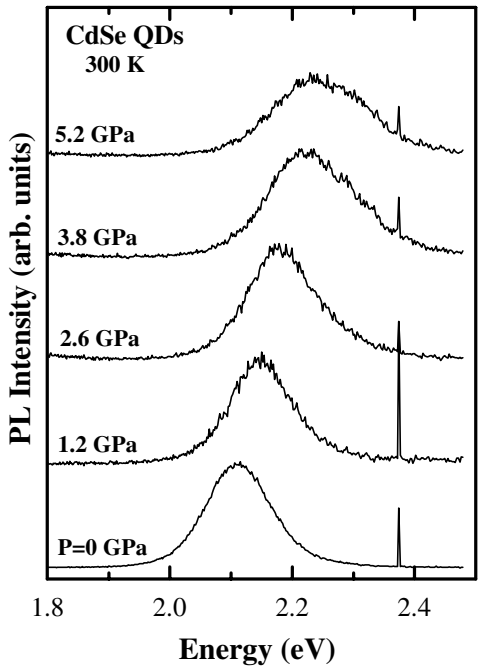

Figure 2. The pressure dependence of the photoluminescence spectra of CdSe nanocrystals at 300 K. The values of the hydrostatic pressure applied in the measurements are marked in the figure.

The previous report [7] found that a phase transition of bulk CdSe from a four-coordinated wurtzite to a six-coordinated rock-salt structure is caused by a pressure of 3.5 GPa, and for CdSe nanocrystal the phase transition pressure monotonically increases with decreasing crystallite size. Consequently, we measured the PL spectra of CdSe nanocrystals under hydrostatic pressure up to 5.2 GPa. We found that the PL peak energies shift linearly with pressure below 5.2 GPa.

Figure 3 shows the pressure dependence of the PL peak energies at room temperature. The linear relation $E^{\Gamma} = E_0 + ap$ is used to fit the experimental data on the pressure dependence, by least-squares fitting. In the formula, E^{Γ} is the PL peak energy at different pressures. E_0 represents the peak energy at atmospheric pressure, p is the applied hydrostatic pressure, and a is the pressure coefficient. The linear relation obtained is $E^{\Gamma} = 2.116 + 0.027$ (eV GPa^{-1}) p for CdSe nanocrystals with the radius of 2.4 nm. The dashed line of figure 3 represents the case of bulk CdSe with the relation $E^{\Gamma} = 1.751 + 0.037$ (eV GPa^{-1}) p (from reference [33]). The calculation of the pressure coefficient will be the focus of the remainder of this paper.

The optical absorption of Cd chalcogenides under pressure was investigated by Edwards and Drickamer [33]. Experiments show that the blue-shifts of the band gap of bulk CdSe and CdS are 37 meV GPa^{-1} and 33 meV GPa^{-1} respectively. Mei and Lemos [34] have reported a blue-shift of 58 meV GPa^{-1} for wurtzite CdSe on the basis of high-pressure photoluminescence measurements. As for the CdSe nanocrystals, Alivisatos *et al* [3] reported measurements on 4.5 nm diameter zinc-blende clusters showing a shift of the absorption onset to higher energy with increasing pressure of 45 meV GPa^{-1}.

First, we calculate the band structure of CdSe (bulk material) under hydrostatic pressure. The parameters concerned are taken from reference [36]: the hexagonal lattice constants $a = 4.30$ Å, $c = 7.02$ Å, the spin–orbit splitting $\Delta_{SO} = 0.42$ eV, and the crystal-field

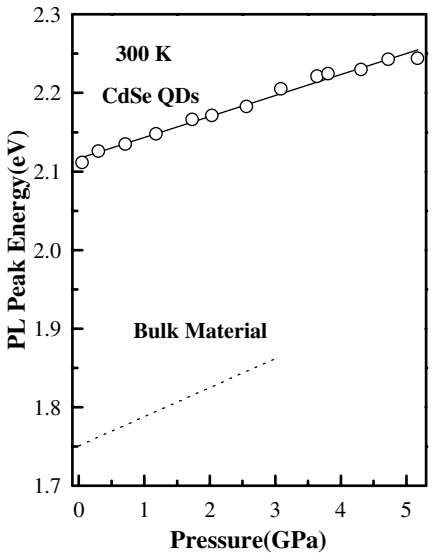

Figure 3. The pressure dependence of the photoluminescence peak energy for CdSe nanocrystals. The solid line represents the result of a least-squares fit to the experimental data with the relation $E^{\Gamma} = 2.116 + 0.027$ (eV GPa^{-1}) p. The dashed line represents the case for CdSe bulk material with the relation $E^{\Gamma} = 1.751 + 0.037$ (eV GPa^{-1}) p (from reference [33]).

splitting $\Delta_c = 40$ meV. The energy bands of wurtzite-type CdSe at 3 GPa obtained by using the pseudopotential method are shown in figure 4. The spin–orbit interaction is not taken into consideration. In order to compare with the result given by Edwards and Drickamer [33], we assume the spin–orbit splitting $\Delta'_{SO} = 0.338$ eV ($<\Delta_{SO} = 0.42$ eV) at 3 GPa for CdSe. As a result, the pressure coefficient of the spin–orbit-splitting energy of CdSe is -27.3 meV GPa^{-1}. Up to now, there has been no work reporting the pressure dependence of Δ_{SO} for CdSe. Consequently, we suggest that further experiments should be done to verify our theoretical results.

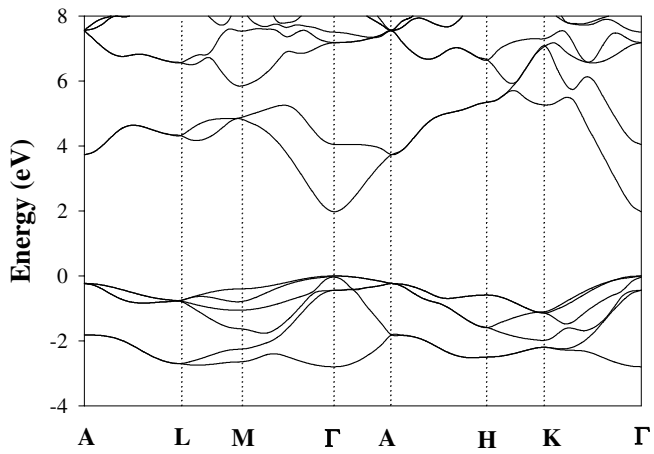

Figure 4. The theoretical electronic band structure at 3 GPa for CdSe material. The spin–orbit interaction is not taken into account in the calculation.

Second, we discuss the relationship between the exciton states and the hydrostatic pressure in CdSe QDs. CdSe QDs can be embedded in different types of material and the values of the electron offset V_e and hole offset V_h for these structures are generally unknown. In this paper, an infinite-potential boundary condition is assumed for the hole calculation, while a finite barrier is used for electrons (V_e). The best fit requires $V_e = 8.0$ eV. It is obvious that this parameter is not physically meaningful, and in practice V_e is used as a fitting parameter.

Table 1 gives the effective-mass parameters of hexagonal CdSe under pressures of $p = 0$ GPa and $p = 3$ GPa. Results for other pressures are also calculated; we do not list them here for the sake of conciseness. Comparing table 1 with reference [26], one sees that the parameters for $p = 0$ GPa are slightly different. This is because in reference [26] we calculated the electronic structure of CdSe nanocrystals at very low temperature ($\sim$10 K) in order to compare with experiments [24], while here the exciton states of CdSe nanocrystallite quantum dots are investigated at room temperature. In the calculation, the pressure coefficient is 26.37 meV GPa^{-1} for the dot radius of 2.4 nm including the Coulomb interaction. This is smaller than that for CdSe bulk materials, 37 meV GPa^{-1} from reference [33]. Furthermore, we find that the pressure coefficients decrease with decreasing dot size in our calculation. Such a phenomenon is similar to those observed for $In_{0.55}Al_{0.45}As$ quantum dots [13, 14] and InAs quantum dots [11]. Obviously the calculated pressure coefficient of 26.37 meV GPa^{-1} is in good agreement with our experimental result shown in figure 3 (27 meV GPa^{-1}). This suggests that the rigid-atomic pseudopotential model is a good approximation in the linear region under pressure.

Table 1. Effective-mass parameters for hexagonal semiconductors under pressures of 0 GPa and 3 GPa.

	m_x	m_z	L	M	N	R	S	T	Q	A
$p = 0$ GPa	0.1669	0.1632	4.9937	0.3485	0.3793	4.6455	0.3643	5.5996	2.5431	0.9253
$p = 3$ GPa	0.1676	0.1646	5.0054	0.3545	0.3897	4.6427	0.3520	5.5706	3.0983	0.7512

In the present calculation, we study CdSe quantum dots under pressure in two steps. First, we calculate the band structure of bulk CdSe under pressure; then we investigate the electronic structure of quantum dots using the second-order-tensors model. The results show that the pressure would chiefly alter the Bloch wave function, while the quantum confinement can have its main effect on the envelope wave function. We plan to calculate the pressure coefficients for other sizes of CdSe quantum dots, and the results will be reported in the future.

5. Conclusions

In this paper, optical spectra of CdSe nanocrystals have been measured at room temperature under pressure ranging from 0 to 5.2 GPa. The exciton energies shift linearly with pressure below 5.2 GPa. The pressure coefficient is 27 meV GPa^{-1} for small CdSe nanocrystals with the radius of 2.4 nm. With the approximation of a rigid-atomic pseudopotential, the pressure coefficients of the energy band are calculated. By using the hole effective-mass Hamiltonian for the semiconductors with wurtzite structure under various pressures, we studied the exciton states and optical spectra of CdSe nanocrystals under hydrostatic pressure in detail. The intrinsic asymmetry of the hexagonal lattice structure and the effect of spin–orbit coupling on the hole states were investigated. The Coulomb interaction of the exciton states was also taken into account. It was found that the theoretical results are in good agreement with the experimental values.

Acknowledgments

This work was supported by the Chinese National Natural Science Foundation. Jingbo Li wishes to thank Professor Yu Lu and Professor Steven G Louie for hospitality and valuable discussions at the International Centre for Theoretical Physics (ICTP) where the theoretical part of this work was started.

References

[1] Brus L E 1984 *J. Chem. Phys.* **80** 4403
[2] Bowen Katari J E, Colvin V L and Alivisatos A P 1994 *J. Phys. Chem.* **98** 4109
[3] Alivisatos A P, Harris T D, Brus L E and Jayaraman A 1988 *J. Chem. Phys.* **89** 5979
[4] Zhao X S, Schroeder J, Persans P D and Bilodeau T G 1991 *Phys. Rev.* B **43** 12 580
[5] Alivisatos A P 1996 *Science* **271** 933
[6] Goldstein A N, Echer C M and Alivisatos A P 1992 *Science* **256** 1425
[7] Tolbert S H and Alivisatos A P 1994 *Science* **265** 373
[8] Tolbert S H, Herhold A B, Johnson C S and Alivisatos A P 1994 *Phys. Rev. Lett.* **73** 3266
[9] Tolbert S H and Alivisatos A P 1995 *J. Chem. Phys.* **102** 4642
[10] Chen C C, Herhold A B, Johnson C S and Alivisatos A P 1997 *Science* **276** 398
[11] Li G H, Goni A R, Syassen K, Brandt O and Ploog K 1994 *Phys. Rev.* B **50** 18 420
[12] Menoni C S, Miao L, Patel D, Micic O I and Nozik A J 2000 *Phys. Rev. Lett.* **84** 4168
[13] Chen Y, Zhang W, Li G H, Han H X, Wang Z P and Wang Z G 2000 *J. Phys.: Condens. Matter* **12** 3173
[14] Chen Y, Li G H, Zhu Z M, Han H X and Wang Z P 2000 *Appl. Phys. Lett.* **76** 3188
[15] Zakharov O, Rubio A and Cohen M L 1995 *Phys. Rev.* B **51** 4926
[16] Fu H X and Zunger A 1998 *Phys. Rev. Lett.* **80** 5397
[17] Empedocles S A and Bawendi M G 1997 *Science* **278** 2114
[18] Xia J B 1989 *Phys. Rev.* B **40** 8500
[19] Murray C B, Norris D J and Bawendi M G 1993 *J. Am. Chem. Soc.* **115** 8706
[20] Ekimov A I, Hache F, Schanne-Klein M C, Ricard D, Flytzanis C, Kudryavtsev I A, Yazeva T V, Rodina A V and Efros Al L 1993 *J. Opt. Soc. Am.* B **10** 100
[21] Efros Al L 1992 *Phys. Rev.* B **46** 7448
[22] Efros Al L, Rosen M, Kuno M, Nirmal M, Norris D J and Bawendi M G 1996 *Phys. Rev.* B **54** 4843
[23] Nirmal M, Norris D J, Kuno M, Bawendi M G, Efros Al L and Rosen M 1995 *Phys. Rev. Lett* **75** 3728
[24] Norris D J, Sacra A, Murray C B and Bawendi M G 1994 *Phys. Rev. Lett.* **72** 2612
[25] Empedocles S A, Norris D J and Bawendi M G 1996 *Phys. Rev. Lett.* **77** 3873
[26] Xia J B and Li J B 1999 *Phys. Rev.* B **60** 11 540
[27] Li J B and Xia J B 2000 *Phys. Rev.* B **61** 15 880
[28] Xia J B 1996 *J. Lumin.* **70** 120
[29] Xia J B, Cheah K W, Wang X L, Sun D Z and Kong M Y 1999 *Phys. Rev.* B **59** 10 119
[30] Schlutter M, Chelikowski J R, Louie S G and Cohen M L 1975 *Phys. Rev.* B **12** 4200
[31] Cohen M L and Heine V 1970 *Solid State Physics* vol 24 (New York: Academic) p 38
[32] Li G H, Jiang D S, Han H X, Wang Z P and Ploog K 1989 *Phys. Rev.* B **40** 10 430
[33] Edwards A L and Drickamer H G 1961 *Phys. Rev.* **122** 1149
[34] Mei J R and Lemos V 1984 *Solid State Commun.* **52** 785
[35] Edmonds A R 1957 *Angular Momentum in Quantum Mechanics* (Princeton, NJ: Princeton University Press)
[36] *Landolt–Börnstein New Series* 1982 Group III, vol 17b, ed O Madelung, M Schultz and H Weiss (Berlin: Springer)